

Effect of Cytokinin and Auxin Treatments on Morphogenesis, Terpenoid Biosynthesis, Photosystem Structural Organization, and Endogenous Isoprenoid Cytokinin Profile in *Artemisia alba* Turra In Vitro

Kalina Danova, Vaclav Motyka, Milka Todorova, Antoaneta Trendafilova, Sashka Krumova, et al.

Journal of Plant Growth Regulation

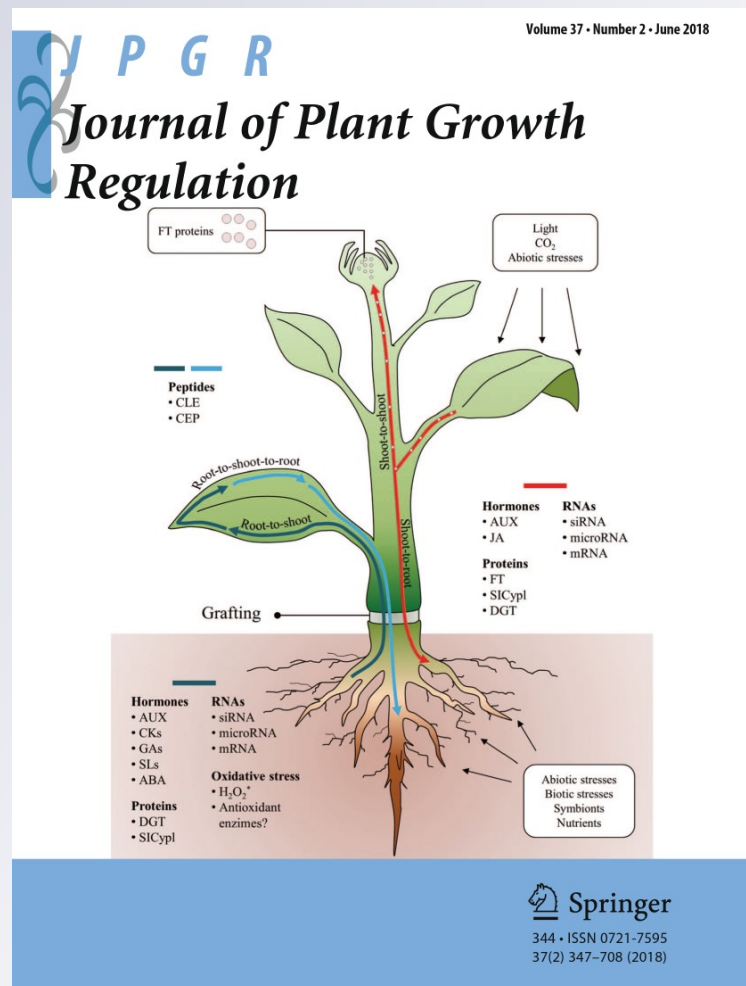
ISSN 0721-7595

Volume 37

Number 2

J Plant Growth Regul (2018) 37:403-418

DOI 10.1007/s00344-017-9738-y



Your article is protected by copyright and all rights are held exclusively by Springer Science+Business Media, LLC. This e-offprint is for personal use only and shall not be self-archived in electronic repositories. If you wish to self-archive your article, please use the accepted manuscript version for posting on your own website. You may further deposit the accepted manuscript version in any repository, provided it is only made publicly available 12 months after official publication or later and provided acknowledgement is given to the original source of publication and a link is inserted to the published article on Springer's website. The link must be accompanied by the following text: "The final publication is available at link.springer.com".

Effect of Cytokinin and Auxin Treatments on Morphogenesis, Terpenoid Biosynthesis, Photosystem Structural Organization, and Endogenous Isoprenoid Cytokinin Profile in *Artemisia alba* Turra In Vitro

Kalina Danova¹ · Vaclav Motyka² · Milka Todorova¹ · Antoaneta Trendafilova¹ · Sashka Krumova³ · Petre Dobrev² · Tonya Andreeva³ · Tsvetelina Oreshkova⁴ · Stefka Taneva³ · Ljuba Evstatieva⁵

Received: 11 January 2017 / Accepted: 29 July 2017 / Published online: 17 August 2017
© Springer Science+Business Media, LLC 2017

Abstract Developmental pattern modification in essential oil bearing *Artemisia alba* Turra was obtained by exogenous plant growth regulator (PGRs) treatments in vitro. Enhanced rooting (in PGR-free and auxin-treated plants) led to elevation of the monoterpeneoid/sesquiterpeneoid ratio in the essential oils of aerals. On the contrary, root inhibition and intensive callusogenesis [combined cytokinin (CK) and auxin treatments] reduced this ratio more than twice, significantly enhancing sesquiterpeneoid production. Both morphogenic types displayed sesquiterpeneoid domination in the underground tissues, which however differed qualitatively from the sesquiterpeneoids of the aerals, excluding

the hypothesis of their shoot-to-root translocation and implying the possible role of another signaling factor, affecting terpenoid biosynthesis. Inhibited rooting also resulted in a significant drop of endogenous isoprenoid CK bioactive-free bases and ribosides as well as CK *N*-glycoconjugates and in decreased *trans*-zeatin (*transZ*):*cis*-zeatin (*cisZ*) ratio in the aerals. Marked impairment of the structural organization of the photosynthetic apparatus and chloroplast architecture were also observed in samples with suppressed rooting. It is well known that in the plant cell monoterpeneoid and *transZ*-type CKs biogenesis are spatially bound to plastids, while sesquiterpeneoid and *cisZ* production are compartmented in the cytosol. In the present work, interplay between the biosynthesis of terpenoids and CK bioactive free bases and

Electronic supplementary material The online version of this article (doi:10.1007/s00344-017-9738-y) contains supplementary material, which is available to authorized users.

✉ Kalina Danova
k_danova@abv.bg

✉ Vaclav Motyka
Motyka@ueb.cas.cz; vmotyka@ueb.cas.cz

Milka Todorova
todorova@orgchm.bas.bg

Antoaneta Trendafilova
trendaf@orgchm.bas.bg

Sashka Krumova
sakrumo@gmail.com

Petre Dobrev
Dobrev@ueb.cas.cz

Tonya Andreeva
t_andreeva@abv.bg

Tsvetelina Oreshkova
tsveti_orehkova@yahoo.com

Stefka Taneva
sgtaneva@gmail.com

Ljuba Evstatieva
luba44@abv.bg

¹ Institute of Organic Chemistry with Centre of Phytochemistry, Bulgarian Academy of Sciences, Acad. G. Bonchev Str., Bl. 9, 1113 Sofia, Bulgaria

² Institute of Experimental Botany, Czech Academy of Sciences, Rozvojová 263, 165 02 Prague 6, Czech Republic

³ Institute of Biophysics and Biomedical Engineering, Bulgarian Academy of Sciences, Acad. G. Bonchev Str., Bl. 21, 1113 Sofia, Bulgaria

⁴ Institute of Biology and Immunology of Reproduction, Bulgarian Academy of Sciences, 73 Tzarigradsko shose, 1113 Sofia, Bulgaria

⁵ Institute of Biodiversity and Ecosystem Research, Bulgarian Academy of Sciences, 2 Gagarin str, 1113 Sofia, Bulgaria

ribosides in *A. alba* in vitro via possible moderation of chloroplast structure has been hypothesized.

Keywords *Artemisia alba* Turra in vitro · *Cis*- and *trans*-zeatin · Endogenous cytokinins · Photosystem II and thylakoid morphology · Plant growth regulators · Terpenoid profile of the essential oil

Introduction

Terpenoids are a wide group of secondary metabolites, with over 40,000 different molecular structures being identified so far (Roberts 2007). Terpenoid-related compounds (some plant hormones, photosynthetic pigments, signal transduction components, defensive molecules, and structural components of the plant cell wall) play a major role in the survival of the plant organism (Mc Garvey and Croteau 1995). In addition, many secondary metabolites with terpenoid chemistry such as the anti-cancer paclitaxel and terpenoid-derived indole alkaloids play a vital role in human health and nutrition. Terpenoids also constitute the chemistry of essential oils, resins, and waxes and are used as raw materials for industry products. Thus, the importance and multiple vital applications of terpenoids impose the challenge of better understanding of their biogenesis in the plant organism. Metabolic engineering of whole plants and plant cell cultures is considered a useful tool for optimizing terpenoid yields and enhancement of flavor, fragrance or color (Roberts 2007). On the other hand, plant cell tissue and organ culture of species with indigenously high terpenoid productivity (such as essential oil bearing plants) represents a simple, convenient, and flexible experimental system for the targeted modification of growth and developmental patterns and elucidation of indigenous factors affecting terpenoid biogenesis in vitro.

Artemisia alba Turra is characterized by a high variability of the terpenoid components in its essential oils, attributed by different authors to environmental, climatic and genetic factors (Radulović and Blagojević 2010 and references cited within). Our previous research on *A. alba* shoot cultures showed that this parameter was strongly affected by the morphogenic changes brought by auxin and cytokinin (CK) treatments in vitro. Although enhanced rooting was related to profound dominance of the monoterpenoids in the essential oils of the aerials, on the contrary, its suppression led to sesquiterpenoid predominance (Danova and others 2012; Danova 2014). Further research was conducted showing that enhanced rooting of *A. alba* in vitro led to elevation of some of the bioactive isoprenoid CKs in the aerials, whereas root

suppression and callusogenesis were characterized by a drop of bioactive isoprenoid CKs and altered fluorescence emission of photosystem II (PSII) (Krumova and others 2013). At this stage of investigations, overlapping of the terpenoid biosynthetic pathways with CK isoprenylation and/or accumulation of the sesquiterpenoids in the aerials of the plants with poorly developed root systems were hypothesized as the possible factors affecting the terpenoid profile of the essential oil of the species.

Though the effects of exogenously applied PGRs on essential oil production in plant cell and tissue culture have been widely explored, to the best of our knowledge up to now no information is available on how endogenous phytohormones might be related to essential oils productivity in vitro.

Root apical meristems are considered the major sites of free CKs biosynthesis (Sakakibara 2006). CKs are then transported acropetally towards the above-ground parts of the plant and further on play vital roles in the different stages of plant development, the cell cycle, as well as in the interactions with such environmental factors as mineral nutrients (especially nitrogenous) (Kakimoto 2003 and references cited therein).

A recent research highlighted for the first time the interrelations between exogenous CK supplementation and PSII functionality of in vitro cultured apple leaves (Dobrąnszki and Mandler-Drienyovszki 2014). It was established that photosystem performance and chlorophyll content responded to the exogenous CK treatment. However, to the best of our knowledge, studies on the relations between endogenous CK levels and PSII response within the whole plant organism are not available in the literature.

Structurally, CKs are adenine derivatives bearing an isoprene or aromatic side chain at the N^6 position (the second type occurring rather rarely in plants). Isoprenoids are common precursors in both terpenoids and CK side chains. The two precursor types isopentenyl diphosphate and dimethylallyl diphosphate are produced by two distinctive biogenetic pathways in plant cells—(1) methylerythriol phosphate (MEP) localized in plastids and responsible for the biosynthesis of *trans*-zeatin (*transZ*) and N^6 -(Δ^2 -isopentenyl)adenine (iP)-type CKs and (2) mevalonate (MVA) localized in the cytosol and leading to *cis*-zeatin (*cisZ*)-type CKs (Kasahara and others 2004). Moreover, in the plant cell, the MEP biogenetic pathway is responsible of monoterpenes synthesis, whereas the MVA pathway leads to sesquiterpenes formation (Bouvier and others 2000).

This motivated us to search for relations between the mono- and sesquiterpenoid production with chloroplast architecture and endogenous isoprenoid CK levels in PGR-treated *A. alba* Turra in vitro model system.

Materials and Methods

In Vitro Cultures of *A. alba*

Shoot cultures were initiated from surface sterilized stem segments of the aerial parts of field grown *A. alba* Turra plants (Danova and others 2012). Five different culture media were used: (a) the control PGR-free (GAIP_0) medium was compared with auxin (indole-3-butyric acid, IBA) either alone or in combination with CK (*N*⁶-benzyladenine, BA) treatments in the following concentrations: (b) 0.5 mg L⁻¹ IBA (GAIP_1); (c) 1.0 mg L⁻¹ IBA (GAIP_2); (d) 0.2 mg L⁻¹ BA + 0.5 mg L⁻¹ IBA (GAIP_3) and (e) 0.2 mg L⁻¹ BA + 1.0 mg L⁻¹ IBA (GAIP_4). *A. alba* shoots were grown for 12 weeks in a plant growth room at 25 °C, 16/8 h photoperiod, irradiation intensity 67 μmol⁻¹ m⁻² s⁻¹ and relative humidity 40%.

Cytokinin Analysis

The freeze-dried samples (equivalent to 9–27 mg dry weight) were extracted and purified according to Dobrev and Kamínek (2002). Stable isotope-labeled internal standards were added to the samples prior to extraction. Two fractions were separated by means of reverse phase and ion exchange chromatography: (1) fraction A containing hormones of acidic and neutral character (auxins, abscisic acid, salicylic acid, jasmonic acid, and gibberellins), and (2) fraction B containing the hormones of basic character (that is, CKs). The CKs were quantified using an HPLC (Ultimate 3000, Dionex, U.S.A.) coupled to hybrid triple quadrupole/linear ion trap mass spectrometer (3200 Q TRAP, Applied Biosystems, U.S.A.) set in selected reaction monitoring mode by using a multilevel calibration graph with internal standards as previously described (Djilianov and others 2013; Žižková and others 2015). Abbreviations for CKs are adopted and modified according to Kamínek and others (2000).

Essential Oil Preparation and GC and GC/MS Analyses

Essential oil was obtained by micro steam distillation–extraction of fresh aerial and underground (root/callus) samples of the in vitro grown plants in a modified Lickens–Nickerson apparatus for 2.5 h (Sandra and Bicchi 1987) using diethyl ether as a solvent. The GC analysis was performed under the experimental conditions reported earlier (Trendafilova and others 2010). The individual components were identified by their retention indices (RI), referring to known compounds described in the literature (Tkachev 2008; Adams 2009), and by co-comparison of their MS with those of NIST 98, as well as with home-made MS databases.

The RI of the oil components were calculated by using the retention times of C8–C22 *n*-alkanes under the same chromatographic conditions.

Isolation and Treatment of Thylakoid Membranes

The thylakoid membrane samples were prepared from 1-h dark- and ice-cold adapted *A. alba* plants as described in Harrison and Melis (1992) and used within 2 h after the isolation. All isolation steps were performed on ice and in dim light. For the spectroscopic measurements, the thylakoid membranes were suspended in medium containing 20 mM tricine (pH 7.8), 5 mM KCl, 5 mM MgCl₂, and 400 mM sucrose (suspension buffer) at a concentration of 15 μg chl ml⁻¹. The chl content was assayed in 80% acetone (v/v) (Arnon 1949).

77 K Steady-State Fluorescence Spectroscopy

77 K chl emission spectra were measured on a Jobin Yvon JY3 spectrofluorimeter upon excitation of 436 nm. The spectra were corrected for the spectral sensitivity of the detection system. Data are presented as the mean of 7–13 independent measurements ± standard error. The data obtained for the GAIP_1–GAIP_4 treatments were normalized to the values obtained for the respective control PGR-free GAIP_0 (measured at the same day as GAIP_1–GAIP_4).

Circular Dichroism

The circular dichroism (CD) spectra of the thylakoid membranes were recorded on a Jobin-Yvon CD6 dichrograph in the range of 400–800 nm (step of 1 nm, integration time of 0.2 s, bandpass of 2 nm, 1 cm optical path length of the cell and 5 cm distance from the photomultiplier to the sample).

Data were collected from four independent measurements and presented as the mean ± the standard error and were normalized to the respective control value determined for GAIP_0.

Flow Cytometry

The flow cytometric analysis was performed by means of an FACSCalibur instrument (Becton Dickinson).

For the proper data selection, the chl fluorescence (originating from intact thylakoids) was discriminated from autofluorescence (due to other membrane bound chromophores) by comparing the fluorescence profiles of the intact and chl-depleted (by acetone extraction of pigments) thylakoids. For the analysis, only the channels representing the chl emission were selected. The samples were excited at 488 nm and the fluorescence was detected above 670 nm. The number of

analyzed objects varied in the range of 20,000–30,000. Due to the small object size, all data are presented in a logarithmic scale.

For the flow cytometric measurements, thylakoid membranes were fixed with 2% (v/v) glutaraldehyde and resuspended in PBS buffer, pH 7.8.

Atomic Force Microscopy

For the atomic force microscopy (AFM) investigation, the isolated thylakoid membranes were resuspended in the 2% (v/v) glutaraldehyde supplied suspension buffer and spread on a freshly cleaved mica surface, covered with 0.01% poly-L-lysine monolayer; 10×10 mm muscovite mica plates (Structure Probe Inc./SPI Supplies, West Chester, PA), fixed to the metal pads. After 20 min of incubation, the samples were rinsed with the suspension buffer and gently dried with a flow of nitrogen gas.

The thylakoid membranes were imaged by a NanoScopeV system, Bruker Inc. atomic force microscope in a tapping mode in air. Silicon cantilevers (Tap300Al-G, Budget Sensors, Innovative solutions Ltd., Bulgaria) with a 30-nm-thick aluminum reflex coating were used (cantilever spring constant 1.5–15 N m⁻¹; resonance frequency 150±75 kHz; tip radius <10 nm). To achieve a high image resolution, the scan rate was set to 0.2 Hz; the topographic, error signal (deflection), and phase images (512×512 pixels) were captured.

The images derived from 7 to 19 individual thylakoids per each of the PGR-treatments were analyzed by NanoScope 6.13R1 software in the following order: first order flattening; roughness analysis; area and height determination applying a 0.00 nm peak threshold value. For area estimation, the objects were approximated to an ellipse. The height of the objects was determined as the difference between the threshold value and the highest object level of the image. The volume of the objects was estimated by the formula for the half-volume of an ellipsoid $V=(4/3\pi abh) 2^{-1}$, where a and b are the short and long axes of the ellipse and h is the height of the thylakoid.

Statistical Analysis

The biological experiment was performed twice, with two independent CK analyses per each. Material was collected of at least 15 individual plantlets, cultivated in 5 separate culture vessels. Comparison of means was conducted by the Student t test for unequal variances. The differences were compared at $P\leq 0.05$.

Results

Developmental Patterns of *A. alba* In Vitro

Two major morphological types were distinguished in relation with their aerial and underground parts development. The first one consisted of clearly differentiated aerial and root parts. These were the plants of the PGR-free control, as well as plants where auxin treatment (IBA) was applied alone (GAIP_0, GAIP_1 and GAIP_2, Fig. 1a–c, respectively). The second group of plants cultured on auxin plus CK (BA) supplemented media, exhibited suppression in rooting and intensive callusogenesis at the explant base (Fig. 1d, e). Indirect rooting through callus was observed in 15–20% of the plants at the end of the cultivation period (Fig. 1f, g). The differences within the first group concerned the formation of primary (>1.10 cm) and secondary (<1.10 cm) axillary shoots when comparing the control (100% only primary shoot formation) with the IBA supplemented plants (54.7 and 60.7% primary shoots, for GAIP_1 and GAIP_2, respectively). Morphological characteristics of *A. alba* in vitro cultures in response to particular PGR treatments were described previously (Danova and others 2012).

Endogenous Isoprenoid Cytokinin Levels

For a better comparative interpretation of the obtained results, data have been presented as a sum of the analyzed CK metabolites, following two criteria: (a) biological function and conjugation as proposed by, for example, Dwivedi and others (2010) and modified with regard to recent data by Lomin and others (2015) (Fig. 2) and (b) chemical structure (Fig. 3). Results have been processed as a percent of the untreated control GAIP_0 (per aerial and underground samples, respectively). To compare the levels of each CK type in the aerial and underground parts, ratios between aerial and roots, and aerial and callus tissues have been also presented (Tables S1 and S2 of the Supplementary material, respectively). The BA-type CK levels are presented in Table S3 (Supplementary material). The contents of all endogenous isoprenoid CKs are shown in Table S4 (Supplementary material).

In vitro rooting (GAIP_0, GAIP_1, and GAIP_2) seemed to be decisive for the high accumulation of endogenous CKs in the aerals, irrespective of the differences of the PGR treatments in these three variants. Thus, as far as biological function/conjugation criterion is concerned, in these plants the levels of bioactive plus transport CKs and CK *N*-glucosides exceeded those of the aerals of plants with inhibited rooting (Fig. 2a, c, e, g). In underground samples, ribotide as well as *N*-glucoside CKs (Fig. 2b, d, respectively) were significantly diminished as a result of the combined BA and IBA treatment in both root and



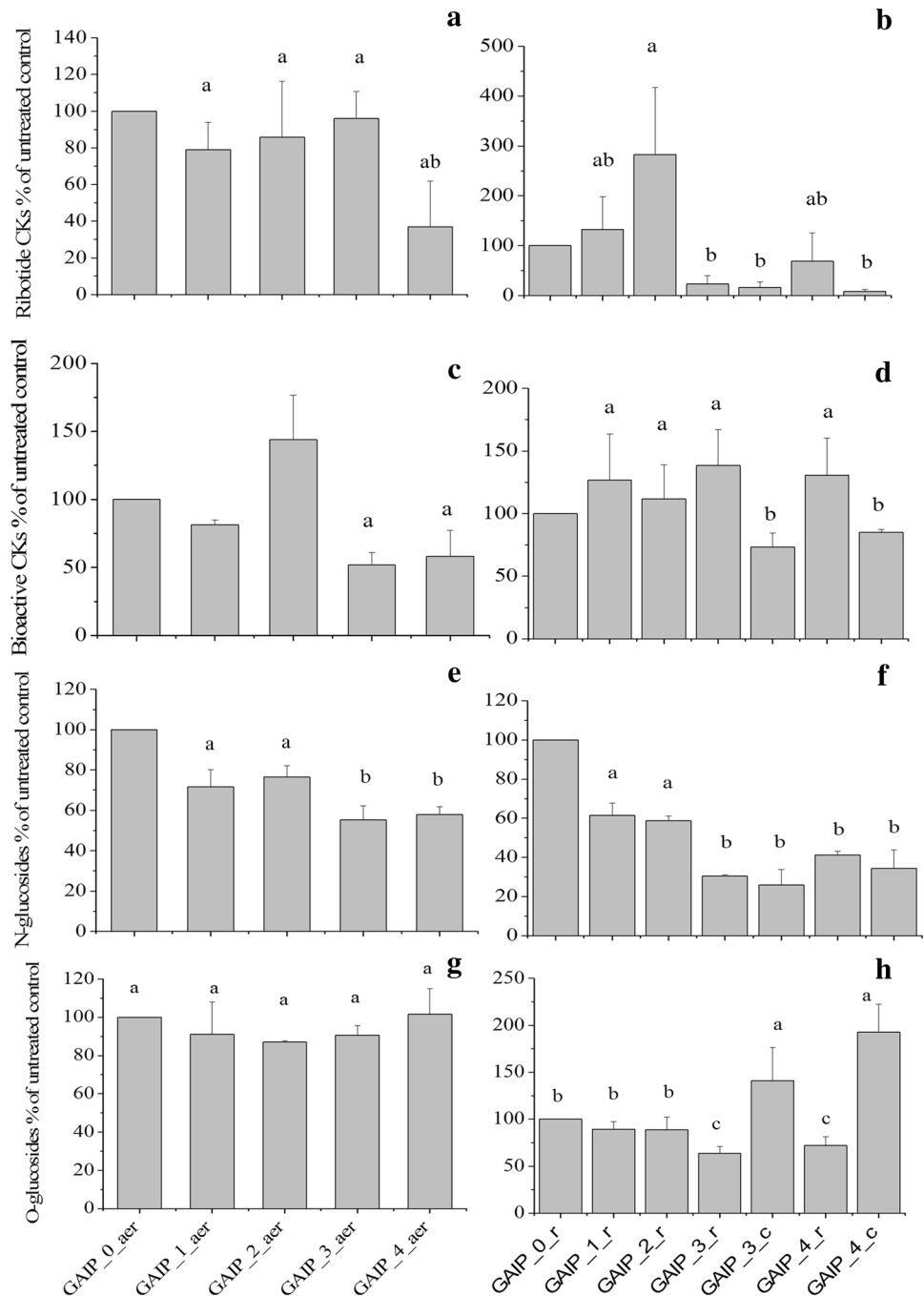
Fig. 1 Effect of PGRs on growth and development of *A. alba* in vitro: **a** PGR-free (GAIP_0) medium (AER aerial parts, DR direct rooting); **b** 0.5 mg L⁻¹ IBA supplemented (GAIP_1) medium; **c** 1.0 mg L⁻¹ IBA supplemented (GAIP_2) medium; **d** 0.5 mg L⁻¹ IBA+0.2 mg L⁻¹ BA supplemented (GAIP_3) medium (CAL cal-

lusogenesis, IndR indirect rooting); **e** 1.0 mg L⁻¹ IBA+0.2 mg L⁻¹ BA supplemented (GAIP_4) medium; Indirect rooting through callus in GAIP_3 (**f**) and GAIP_4 (**g**) supplementations. IBA = indole-3-butyric acid; BA = N⁶-benzyladenine. Space bar 1 cm

callus tissues as compared with the PGR-free control. As far as endogenous CK free bases and riboside levels in underground tissues are concerned, they were lowered only in the callus tissues of the respective treatments

(Fig. 2d, callus samples of GAIP_3 and GAIP_4). On the other hand, remarkable stimulation of *O*-glucoside CKs was recorded in the callus tissues of GAIP_3 and GAIP_4 plants.

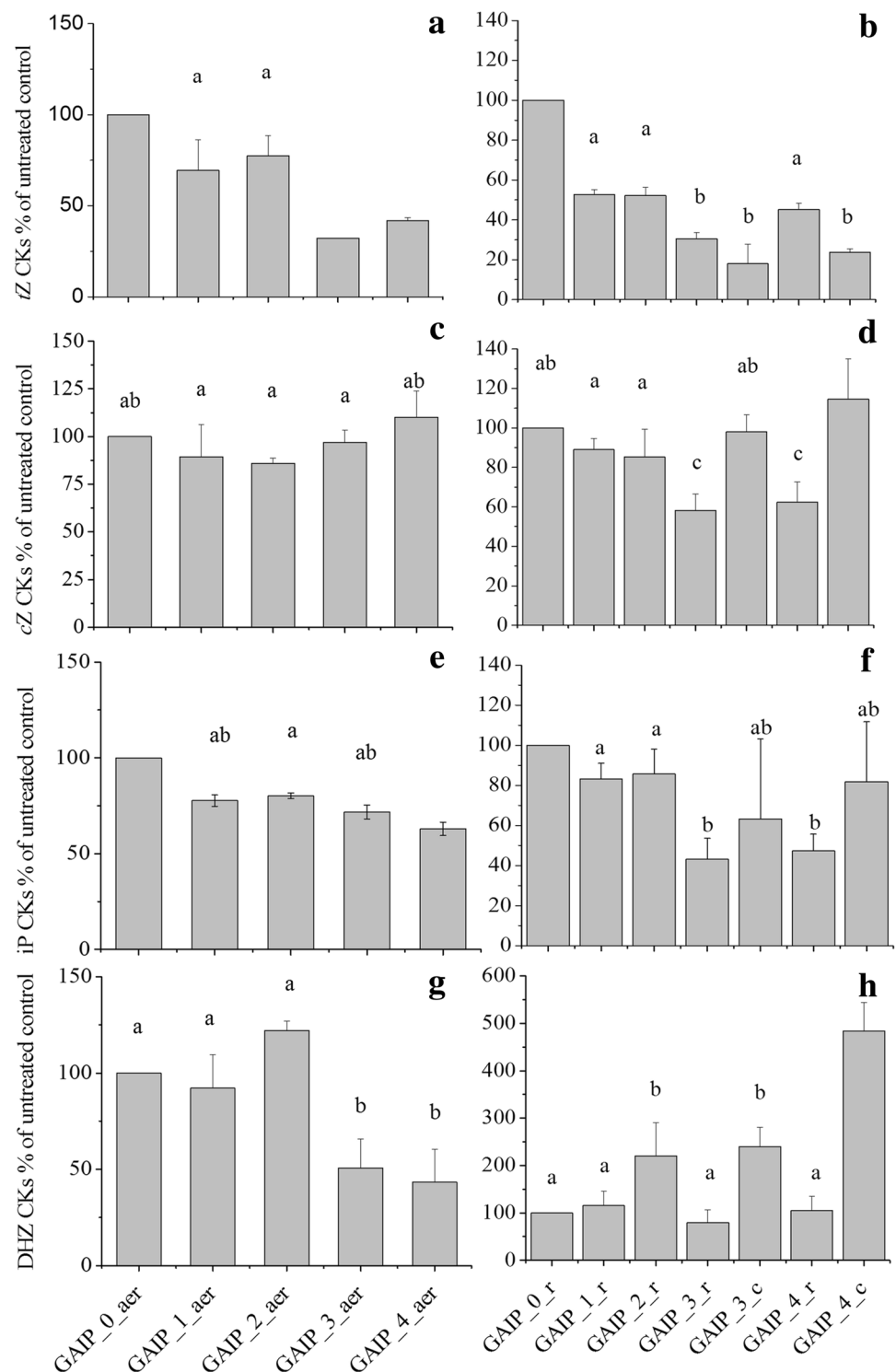
Fig. 2 Sum of isoprenoid cytokinins organized by biological function/conjugation status criteria. Ribotides in aerial (**a**) and underground (**b**); cytokinin-free bases and ribosides in aerial (**c**) and underground (**d**); *N*-glucosides in aerial (**e**) and underground (**f**); *O*-glucosides in aerial (**g**) and underground (**h**) samples of the plant. Values are presented as a percent of the untreated control (GAIP_0). *aer* aerial, *r* roots, *c* callus samples. The biological experiment was performed twice, with two independent CK analyses per each. The concentrations of all individual isoprenoid cytokinins are presented in Table S4. *Same letters* denote insignificant differences



Then, regarding the chemical structure data processing, a marked difference in the response of *transZ* and *cisZ* CK types was established for both aerial and underground samples (Fig. 3a–d). Thus, although callus formation (GAIP_3 and GAIP_4 treatments) was related to a drop of the *transZ*-type CKs in both aerial and underground samples (Fig. 3a, b), the levels of *cisZ* types in the aerials were not significantly influenced by the morphology of the plants of the different treatments (with the only exception of stimulation of *cisZ* levels in GAIP_4 aerials).

Interestingly, in both types of data processing, a drop of certain CKs such as *transZ* types in the callus (as compared with the root tissue) was always related to a drop of their levels in the aerials (bioactive plus transport as well as *N*-glucoside CKs, Fig. 2d, f, respectively). On the other hand, the opposite was found for other CK derivatives such as *O*-glucosides and *cisZ* types, prevailing in the callus (as compared with roots) and also occurring in high concentrations in the aerials. This observation might be indicative of the better callus-shoot, as compared with

Fig. 3 Sum of isoprenoid cytokinins organized by chemical structure criteria. *transZ*-type cytokinins in aerial (a) and underground (b); *cisZ*-type cytokinins in aerial (c) and underground (d); iP-type cytokinins in aerial (e) and underground (f); DHZ-type cytokinins in aerial (g) and underground (h) samples of the plant. Values are presented as a percent of the untreated control (GAIP_0), *aer* aerial, *r* roots, *c* callus samples. The biological experiment was performed twice, with two independent CK analyses per each. The concentrations of all individual isoprenoid cytokinins are presented in Table S4. Same letters denote insignificant differences. *transZ* = *trans*-zeatin, *cisZ* = *cis*-zeatin, iP = N⁶-(Δ^2 -isopentenyl) adenine, DHZ = dihydrozeatin



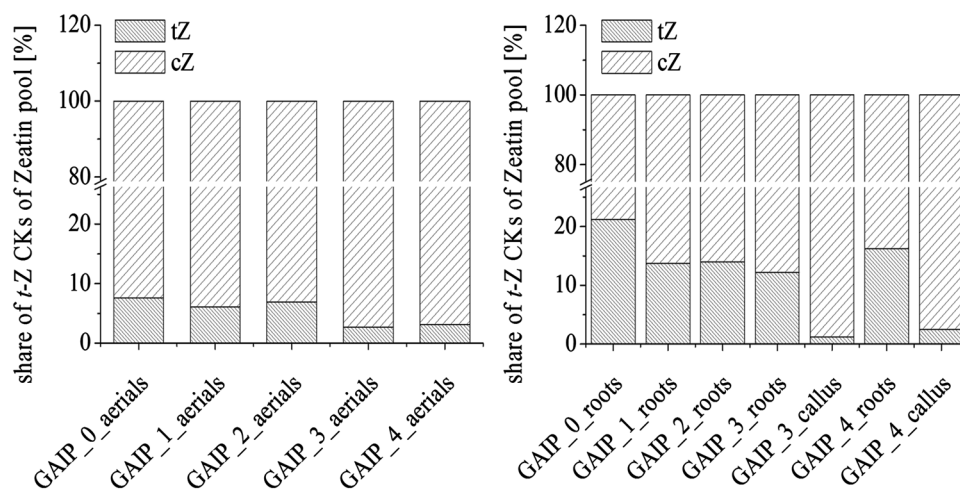
root-shoot, communication in GAIP_3 and GAIP_4 where roots were formed only rarely indirectly through callus.

In addition to these observations, noteworthy is the share of *transZ* CKs in the *transZ/cisZ* pool significantly dropped in the callus of GAIP_3 and GAIP_4 plants (Fig. 4).

Terpenoid Profiles of the Essential Oils of Aerial and Underground Parts of *Artemisia alba* In Vitro

Comparison of the terpenoid profiles of the different PGR-treatment samples was made based on 22 components in the aerials (Table 1), and 16 components in the underground

Fig. 4 Distribution between the endogenous levels of *cis*- and *trans*-zeatins (the total content of all *cis*- and *trans*-zeatin derivatives = 100%). The concentrations of individual zeatin derivatives are shown in Table S4 (Supplementary material)



samples (Table 2) of the plant. The Tables represent the concentrations of components, exceeding 0.5% in the respective oils. Components 1–6 (Table 2) have not been identified, but based on their MS data (molecular mass and fragmentation) they have been characterized as sesquiterpenoids. The main constituents in the aerial parts were predominantly monoterpenoids, mostly *O*-containing irregular ones such as yomogi alcohol, artemisia alcohol, and artemisia acetate (of the

monoterpenoid components). Unlike for monoterpenes, sesquiterpenes were predominantly present in the carbohydrate form, germacrene-D being the most abundant component. PGRs treatment generally increased the content of yomogi alcohol and germacrene-D and decreased the amounts of artemisia alcohol and artemisia acetate of all PGR-treated plants as compared with the GAIP_0 control (Table 1). The dominating components in the oils of the underground parts

Table 1 Terpenoid profile of the essential oils of the aerial parts of *Artemisia alba* Turra as a results of PGR treatments

RI	Component (%)	Terpenoid type	GAIP_0	GAIP_1	GAIP_2	GAIP_3	GAIP_4
1000	Yomogi alcohol	IMO	30.4	35.7	35.3	35.7	36.6
1037	1,8-Cineole	MO	0.4	0.5	0.5	t	t
1085	Artemisia alcohol	IMO	13.7	12.9	13.1	10.9	10.2
1114	Fenhol-endo	MO	0.9	0.9	1	1.9	0.8
1139	5,6-Epoxyartemisia ketone	IMO	0.9	0.9	1	0.7	t
1140	Trans-verbenol	MO	1	1.1	1.4	0.6	0.5
1141	Camphor	MO	1.5	1.6	2.3	0.9	1.3
1171	Pinocarvone	MO	0.6	0.6	0.5	t	t
1173	Artemisia acetate	IMO	28.3	20.7	22.6	18.0	12.3
1174	Borneol	MO	0.9	0.7	0.6		
1197	α -Terpineol	MO	0.6	1.3	1.2		0.5
1287	Linalool oxide acetate (pyranoid)	MO	1	1.1	1.1	0.4	0.8
1292	M=152	MO	1	1.1	1.1	0.4	1.2
1310	Unidentified	MO	1.2	1.5	1.3	0.7	1.2
1349	β -Elemene	S	1.2	1.1	1	1.1	1.6
1460	Trans- β -farnesene	S	1.1	1	1	4.4	5.1
1492	Germacrene D	S	7.1	7.3	7.9	13.9	16.8
1505	Bicyclogermacrene	S	0.6	0.6	0.7	1.2	1.1
1560	Elemol	SO	3	2.8	2.5	2.8	2.6
30.9	M=220	SO	0.8	0.8	0.8	1.2	1.2
1696	Elemol acetate	SO	1.2	1.2	1	1.2	1.1
1775	M=222	SO	0.8	0.7	1.1	2.2	3.5

The table represents concentrations of components exceeding 0.5% of the total in the respective oils

RI retention index, IMO irregular oxygenated monoterpenes, SO oxygenated sesquiterpenes, M monoterpenoids, S sesquiterpenoids

Table 2 Terpenoid profile of the essential oils of the roots of *Artemisia alba* Turra as a results of PGR treatments

RI	Component (%)	Terpenoid type	GAIP_0	GAIP_1	GAIP_2	GAIP_3	GAIP_4
1000	Yomogi alcohol	IMO	0.9	1	0.9	4.8	7.6
1085	Artemisia alcohol	IMO	tr	0.5	0.2	0.8	1
1173	Artemisia acetate	IMO	tr	tr	tr	0.8	0.5
1349	β -Elemene	S	4.8	5.8	6.2	11.3	7.3
1460	Trans- β -farnesene	S	2.8	2.3	2.3	2.4	2.6
1483	γ -Himachalene	S	18	15.6	13.4	10.3	6.8
1487	β -Selinene	S	0.5	0.7	0.8	0.7	
1522	δ -Cadinene	S	0.7	0.8	0.6	tr	
1560	Elemol	SO	tr	tr	tr	0.6	
1617	M_220 (1)	SO	16.2	18	13.6	10.3	8.8
1630	1-Epi-cubenol	SO	0.7	0.7	0.4	tr	
1996	M_220(2)	SO	5.8	7.2	6.3	4.5	3.5
1710	M_220(3)	SO	0.8	0.8	0.8	0.5	
1715	M_262(4)	SO	23	24.8	27.7	23.7	21.6
1731	M_220(5)	SO	7.5	5.6	5.1	3.7	3.2
1770	M_220(6)	SO	1	1.2	1	0.5	t

The Table represents concentrations of components exceeding 0.5% of the total in the respective oils

RI retention index, *IMO* irregular oxygenated monoterpenes, *SO* oxygenated sesquiterpenes, *M* monoterpenoids, *S* sesquiterpenoids

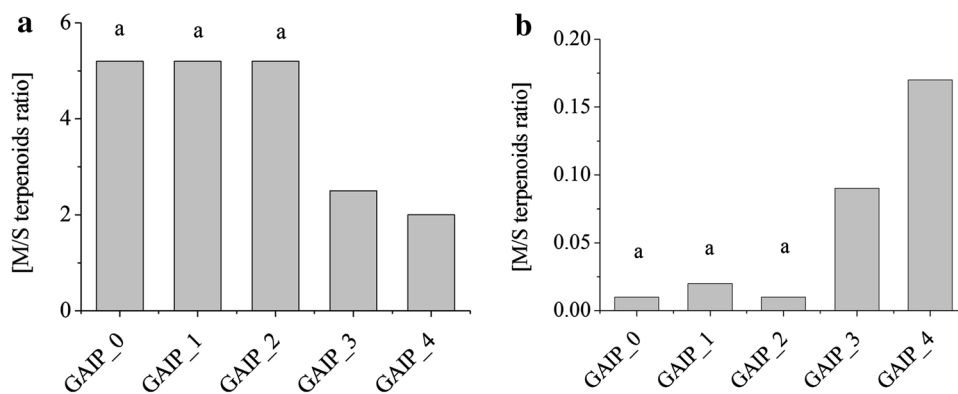
were β -elemene, *trans*- β -farnesene and γ -himachalene, as well as unidentified components with structures of oxygenated sesquiterpenes (compounds 1, 2, 4, and 5). In general, in the underground parts, all PGR treatments increased the contents of artemisia alcohol, yomogi alcohol, and β -elemene and decreased those of γ -himachalene and compound 5 as compared with the PGR-free control (Table 2).

As obvious from Fig. 5, the monoterpenoid/sesquiterpenoid ratio in the oils of the aerials of GAIP_0, GAIP_1, and GAIP_2 (samples with developed root system) was 2X higher than that in GAIP_3 and GAIP_4 (samples with inhibited rooting and callusogenesis at the base of the shoot clumps).

As a general observation, sesquiterpenoids (mostly oxygenated) prevailed over monoterpenoids in the oils of the underground parts (Table 2; Fig. 5). Compounds 1, 2,

4, and 5 predominated with 4 being the basic one, reaching up to 27.7% in GAIP_2. Of the monoterpenoids, only yomogi alcohol, artemisia alcohol, and artemisia acetate (basic components in the aerials) have been identified in the roots. When systematizing the data of the terpenoid profiles of the oils of underground parts, two main plant groups were also confirmed here. Thus, in GAIP_0, GAIP_1, and GAIP_2 monoterpenoids reached up to 1.5% of the total, their content in GAIP_3 and GAIP_4 increased up to 6.4 and 9.1%, respectively (Table 2). As far as sesquiterpenoids (S) are concerned, the root samples displayed a significantly higher content (81.8, 83.5, and 78.2% S total, for the oils of GAIP_0, GAIP_1, and GAIP_2 undergrounds, respectively), as compared with callus samples (68.5 and 53.8% S total, for the oils of GAIP_3 and GAIP_4 undergrounds, respectively). These two tendencies led to a much higher monoterpenoid/

Fig. 5 Total monoterpenoid/sesquiterpenoid (M/S) ratios in the essential oils of aerial (a) and underground parts (b) of in vitro cultivated *Artemisia alba*. For the source data see Tables 1 and 2 and Krumova and others (2013)



sesquiterpenoid ratio in oils of the callus samples (GAIP_3 and GAIP_4 underground parts), as compared with GAIP_0, GAIP_1, and GAIP_2 root oils (Table 2; Fig. 5). This observation was indicative of the higher capacity of callus as compared with root tissue to produce monoterpenoids.

Photosystem II Structural Organization in *A. alba* In Vitro

The photosynthetic (thylakoid) membrane represents a highly complex protein-enriched network compartmentalized into stacked regions (granas), abundant in photosystem II (PSII) and unstacked stromal lamellae, enriched in photosystem I (PSI) (Albertsson 2001; Pribil and others 2014).

To probe the global architecture of the thylakoid membranes, flow cytometry and atomic force microscopy (AFM) were combined. The side scatter (SSC) versus front scatter (FSC) profiles recorded for the GAIP_0–GAIP_4 PGR-modifications by flow cytometry are presented in Fig. 6a. Two regions in the SSC versus FSC plots were defined corresponding to fractions with small (F_S) and large (F_L) dimensions (based on the assumption that large scattering originates from large objects) and their relative contribution ($F_S:F_L$ ratio) was estimated. All PGR treatments showed higher abundance of small objects, more pronounced for GAIP_1 and GAIP_2 (by 27 and 44%, respectively), than for GAIP_3 and GAIP_4 (by 15 and 25%, respectively) (Fig. 6a). It was also noticed that the relative contribution of small objects was higher

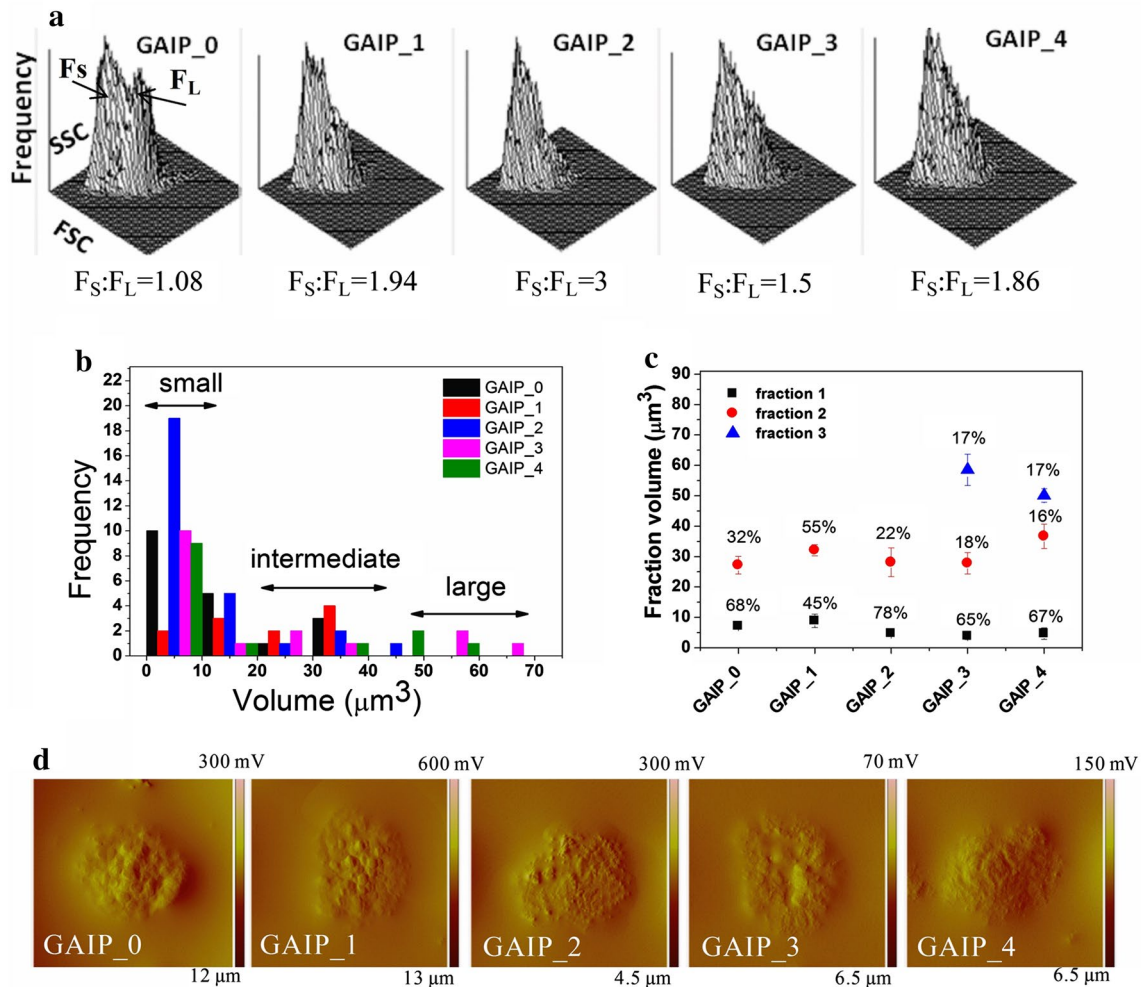


Fig. 6 Alterations in plastid morphology of the studied GAIP variants. **a** Characteristic SSC versus FSC profiles of the different GAIP variants recorded by FACS and ratios between the small and large objects ($F_S:F_L$). **b** Histogram of thylakoids volume determined by atomic force microscopy (AFM); three fractions (denoted by arrows) are defined based on similarity in volume. **c** Mean volume (\pm SE) of

each fraction and its relative abundance (% from the total number of objects recorded for each variant). **d** Typical AFM tapping mode error images of GAIP thylakoids, note the different vertical and horizontal scales. The bright circular objects (nicely resolved in GAIP_0 and GAIP_1 and smeared in GAIP_3 and GAIP_4) represent individual granas

for GAIP_2 than for GAIP_1, and for GAIP_4 than for GAIP_3, thus the increase in the applied concentration of auxin IBA (either alone or in combination with CK BA) correlated with decreased large thylakoids abundance. Due to the small size of the thylakoid membranes, more details on their morphology such as the number of membranes in a granum stack and the lateral size of the grana and stroma lamellae contributing to the specific size and shape of the thylakoids could not be discriminated by flow cytometry. Besides, these parameters are not uniform among the different chloroplasts, not even within a single chloroplast, but vary in a wide range. Therefore, a main disadvantage of the flow cytometry measurements is the lack of quantitative information. To overcome this obstacle, AFM was performed allowing estimation of the thylakoids volume and helping to draw conclusions about the general morphological characteristics of the thylakoids in the GAIP_0–GAIP_4 treatments.

The thylakoid volume histograms established for the particular variants revealed three populations of thylakoids (Fig. 6b). The mean volume of the resolved fractions for each *A. alba* treatment is plotted in Fig. 6c. The dominant fraction (68%) for GAIP_0 had a mean volume of $7.2 \mu\text{m}^3$; this fraction dropped to 45% for GAIP_1. For all other variants, the main fraction was 2 times lower in volume (3.6 – $4.7 \mu\text{m}^3$). Similar to flow cytometry data, this small thylakoid fraction was more abundant in GAIP_2 than in GAIP_1 as well as in GAIP_3 compared to GAIP_4 (Fig. 6c).

All treatments with the exception of GAIP_2 contained a fraction with a volume of 27 – $36 \mu\text{m}^3$, which was the most abundant in GAIP_1 (55%). Only GAIP_3 and GAIP_4 had an additional fraction with a volume larger than $40 \mu\text{m}^3$, accounting for 17% of the total number of analyzed objects (Fig. 6c). Thus, the latter population of thylakoids must be related to the addition of BA in the growth medium and by the corresponding changes in the developmental patterns of *A. alba* in these treatments.

To explore the grana morphology and its dependence on the applied PGR treatment, the AFM images were recorded at higher magnification. The typical topographic images of the thylakoids from the most abundant population for each variant (fraction 1 for GAIP_0, GAIP_2, GAIP_3, and GAIP_4 and fraction 2 for GAIP_1) are shown in Fig. 6d. Well-defined grana with sizes on the order of 550 – 750 nm , typical for a variety of plant species (Pribil and others 2014 and references therein), were observed for GAIP_0. Grana of similar dimensions were also observed for GAIP_1; however, additionally larger structures with smeared edges and smaller granular objects were also recognized. These granules were highly enriched in GAIP_2 thylakoids. The grana edges were hardly visible for GAIP_3 and completely featureless for GAIP_4 (Fig. 6d). Thus, the obtained data indicated that all PGR-treated variants possess altered grana

morphology, with sharp differences observed for GAIP_3 and GAIP_4 plants.

Having demonstrated the strong dependence of the overall thylakoid structure on the applied PGRs, further investigations aimed to elucidate whether this effect was accompanied by structural changes affecting the PSII integrity (by means of 77 K fluorescence) and lateral organization (by circular dichroism, CD). Two characteristic fluorescent ratios were determined—the $F_{695/686}$ ratio as an indicator of possible structural changes in the PSII components (the fluorescent band at 695 nm originates from CP47 emission and that at 686 nm from energy transfer towards the reaction center of PS II antenna, respectively) and the $F_{730/686}$ ratio, as a marker for the excitation energy distribution between the two photosystems (the fluorescent intensity at 735 nm is due to PSI while that at 686 nm originates from PSII, respectively) (Mullet and others 1980; Dekker and others 1995; Gobets and van Grondelle 2001; Andrizhivskaya and others 2005). The $F_{695/686}$ ratio was significantly lower for all PGR treatments as compared with the control (Fig. 7a). Interestingly, the decrease was more pronounced in GAIP_1 than GAIP_2 and in GAIP_3 than GAIP_4, indicating again a stronger effect caused by the higher auxin concentration. It should be noted that the reduction in $F_{695/686}$ was not higher than 15% (for GAIP_3 and GAIP_4) and hence can rather be attributed to the small structural changes affecting the energy transfer within the PSII core complexes, than to major structural alteration that would significantly affect PSII functionality. Large variations were found for the $F_{730/686}$ parameter for GAIP_2, GAIP_3, and GAIP_4 variants (data not shown); only GAIP_1 exhibited a significantly lower (by 11–24%) $F_{730/686}$ ratio compared to the GAIP_0 control suggesting lower functional activity of PSII in this variant or somewhat lower PSI content. To clarify this point, functional characterization of the different PGR-treatments would be highly informative.

Next, we investigated the change in the intensity of the 689/673 circular dichroism (CD) band in the different PGR treatments because this parameter has been shown to be proportional to the extent of the lateral order of PSII in the thylakoid membrane (Kovács and others 2006). The intensity of the 689/673 CD band was very similar for GAIP_0 and GAIP_1 and slightly lower for GAIP_2 (Fig. 7b). However, it significantly decreased (by about 25% of the control value) for GAIP_3 and GAIP_4 treatments (Fig. 7b) revealing a reduced order of PSII in CK-treated plants in comparison to CK-untreated ones (GAIP_0, GAIP_1, and GAIP_2).

Discussion

By playing a central role in the plant cell cycle, CKs fundamentally influence plant growth and development. They

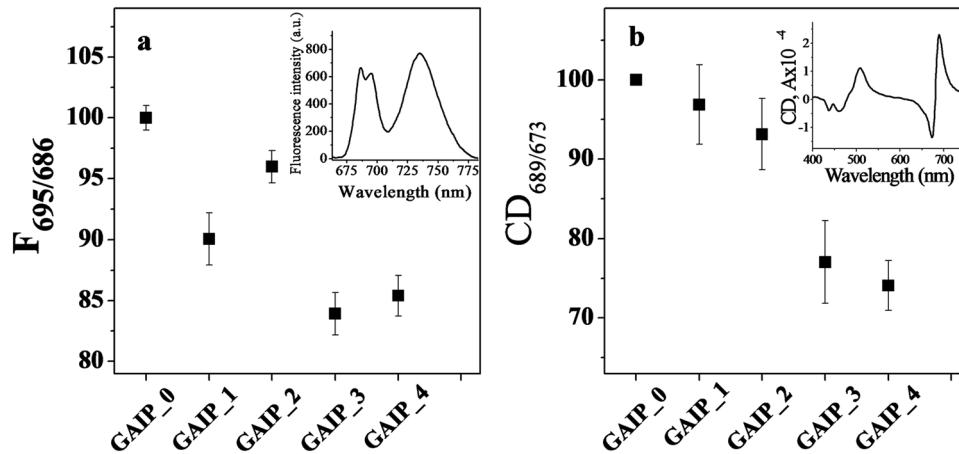


Fig. 7 Characterization of PSII integrity by 77 K fluorescence (a) and lateral order by means of circular dichroism (b). $F_{695/686}$ ratio (mean \pm SE) determined for thylakoid membranes emission spectra recorded at 77 K upon 436 nm excitation; *inset* selected 77 K emission spectrum of GAIP_0 thylakoid membrane recorded upon 436 nm

excitation (a). Intensity of the 689/673 nm circular dichroism (CD) band (mean \pm SE) determined for the GAIP_0–GAIP_4 variants; *inset* characteristic CD spectrum recorded for GAIP_0 thylakoids (a). The data are presented as a percentage of the value obtained for GAIP_0

have been shown to be important regulatory factors of plant meristem activity and morphogenesis, with opposing roles in shoots and roots (Werner and others 2003). Thus, transgenic tobacco plants with reduced endogenous CK levels (resulting from the genetically engineered CK oxidase/dehydrogenase expression) have shown a retardation of shoot growth and underdevelopment of apical meristems on one hand, and leaf cell production only 3–4% of that of the wild type. On the other hand, root meristems of transgenics were enlarged, giving faster growing and branched roots (Werner and others 2001).

Our results indicated that even a low exogenous CK supplementation (0.2 mg L^{-1} BA) affected *A. alba* in vitro morphogenesis by a strong inhibition of root formation, irrespective of the variation of auxin concentrations (0.5 and 1.0 mg L^{-1} IBA).

It is well known that exogenously supplied PGRs strongly affect patterns of plant growth and development in vitro. Logically PGR treatments have an impact on endogenous phytohormone homeostasis in the plant through multiple mechanisms, that might possibly be feed-back regulation, or by altering the morphological structures of the plant thus secondarily affecting endogenous phytohormone pools. Therefore, we were motivated to further explore the endogenous CK balance in the obtained in vitro culture systems of *A. alba*.

Thus, the morphological patterns of the underground parts seemed to be decisive for the endogenous isoprenoid CK profile of the plants, rather than the different concentrations of PGRs in the particular experimental treatments. In addition, the present results strongly indicate that in the case of suppressed direct rooting the callus tissue seems to

be responsible for the production and delivery of isoprenoid CKs towards the aerial parts.

Under physiological conditions, callus tissue is produced by the plant organism as a response to exogenous stress stimuli such as wounding and/or pathogen infection (Ikeuchi and others 2013). Induction of callus can also be achieved (and is widely utilized for fundamental and practical applications) by modifying the PGR regime in vitro (most often auxin/CK ratio). The ratio between these two types of PGRs determines the state of dedifferentiation in the tissue (Skoog and Miller 1957). To the best of our knowledge, whereas many studies have been dedicated to the effect of exogenously supplied auxins and CKs on the response of different explant types, less literature findings are available regarding the variations within the endogenous CK pools of differentiated (shoots and roots) and non-differentiated (callus) tissues functioning integrally into one and the same plant individual.

Recent research sheds light on the cross-talk between shoot- and root-derived CKs in the overall synchronization of plant development. It is known that CKs of the *transZ*-type are mainly synthesized in root vascular tissues and are then translocated to the shoots where they play a role in shoot growth regulation (Ko and others 2014). It is also known that CK translocation is conducted via the xylem tissues (Kudo and others 2010). Then, it has been additionally established that the *iP*-type CKs are the predominant CK types in the phloem being translocated from the aerial tissues to the roots and responsible for developmental patterns of the latter tissue (Hirose and others 2008; Bishopp and others 2011). The phloem predominance of *iP*- and *cisZ*-type CKs has been hypothesized to be an indicator of the

latter as functioning as a basipetal or systematic signal in the plant organism (Hirose and others 2008 and references cited within). In addition, it has been demonstrated that in the *Arabidopsis* mutant lacking ATP-binding cassette transporter responsible for root-to-shoot CK translocation, the accumulation of high *transZ* levels in the roots led to characteristic disturbances of the growth and development of the aerial tissues (Ko and others 2014). Moreover, literature data show that high *cisZ/transZ* ratios are characteristic of lower non-vascular plants (algae, fungi, mosses, and so on) (Gajdošová and others 2011; Závěská Drábková and others 2015, and references therein).

The observations of the present experiment might be indicative of the reduced efficiency of root-to-shoot CK transport in *A. alba* in vitro of GAIP_3 and GAIP_4 roots (formed indirectly through callus) to supply CKs to the respective aerial tissues of the plant, possibly due to the lack of proper vascular structures necessary for the conduction of such transport.

Adenosine phosphate-isopentenyltransferase (IPT) is a key enzyme in CK biogenesis catalyzing the prenylation of adenosine phosphate using dimethylallyl diphosphate (DMAPP) as an isoprene donor (Takei and others 2004). Prenylation of the side chain of CKs is a bottleneck in their biogenesis. The common isoprenoid precursors isopentenyl diphosphate (IPP) and DMAPP are produced by two alternative pathways in plant cells, by (1) the methylerythritol phosphate (MEP) pathway localized in plastids and giving rise to *transZ*- and *iP*-type CKs and (2) the mevalonate (MVA) pathway in the cytosol providing *cisZ* types (Kasahara and others 2004).

Thus, isoprenoids represent common precursors of both CK and terpenoid biogenesis, which motivated us to search for alterations of the terpenoid profile of *A. alba* by the different PGR treatments.

In general, similarly to the parameters discussed above, the determining factor for mono- and sesquiterpenoid production in the aerials and their respective underground parts seemed to be the exogenous application of CK (BA) to the medium and its effect on plant morphogenesis (inhibition of root formation). Thus, the individual auxin (IBA) treatments (GAIP_1 and GAIP_2) did not significantly affect the qualitative and quantitative characteristics of *A. alba* essential oils (moreover, these plants were similar to the PGR-free control).

The observed relations between the drop of sesquiterpenoids, and at the same time the elevation of endogenous CKs such as bioactive plus transport, as well as *N*-glucoside forms in the aerials of GAIP_0, GAIP_1, and GAIP_2 impose the question of a possible overlapping of terpenoid biosynthetic pathways and isoprenylation of CKs as a factor affecting terpenoid biogenesis of the essential oils of the species.

Interestingly, the distinctive responses of the *cisZ*- and *transZ*-type CKs were also dependent on the two groups of plants. As discussed above, the biogenetic pathways of monoterpenoids and the MEP pathway leading to the prenyl group of *transZ* types are spatially bound to the plastids, whereas sesquiterpenoid biogenesis and the MVA pathway responsible for the formation of the *cisZ* prenyl group are committed to the cytosol of the cell (Bouvier and others 2000; Kasahara and others 2004).

This led us to investigate the response of the photosynthetic membrane embedded in the chloroplast (in terms of structural modifications) with the aim to search for possible alterations of the chloroplast architecture which might be related to the observed alterations of the levels of the metabolites whose biogenesis is spatially bound to the chloroplast.

The lateral organization as well as the functionality of the two photosystems is affected by a multitude of endogenous and exogenous factors. So far multilevel links between the operation of the photosynthetic complexes and the biosynthesis of monoterpenoids have been identified: (i) spatial relationship—both processes take place in the chloroplasts, (ii) precursor supply—the carbon reactions of photosynthesis provide building blocks for terpenes biosynthesis, (iii) reductive power—electron transport in the thylakoid membranes provides reductive molecules needed for the functioning of some of the MEP enzymes (Seemann and others 2006).

Though representing secondary metabolites in their chemical nature, plant hormones have a vital primary role in plant growth and development and are ubiquitous in the plant kingdom. They represent a physiological mediator responsible for harmonized functioning of the living plant and their endogenous regulation is a subject of interrelations between the plant organism and the factors of its environment. As well known, due to their attached way of life, plants respond to environmental challenges by production of secondary metabolites, which are not directly engaged in their growth and development. The building blocks of plant secondary metabolites arise from different branches of primary metabolic pathways (Bajaj and others 1998). Little is still known on the interplay between secondary metabolite production and endogenous hormonal regulation of plants. A work of Chu and others (2011) shows that for all five plant secondary metabolic gene clusters reported so far the enzymes catalyzing the first committed steps are most probably recruited from primary metabolic pathways involved in phytohormone synthesis.

The experimental set-up of the PGR-treatment of *A. alba* shoot cultures in the present work has led to the development of two distinctive in vitro systems: plants from the first one (PGR-free control and 0.5 and 1.0 mg L⁻¹ IBA treated plants) were characterized with the development of both aerial parts and a root system. The second in vitro system

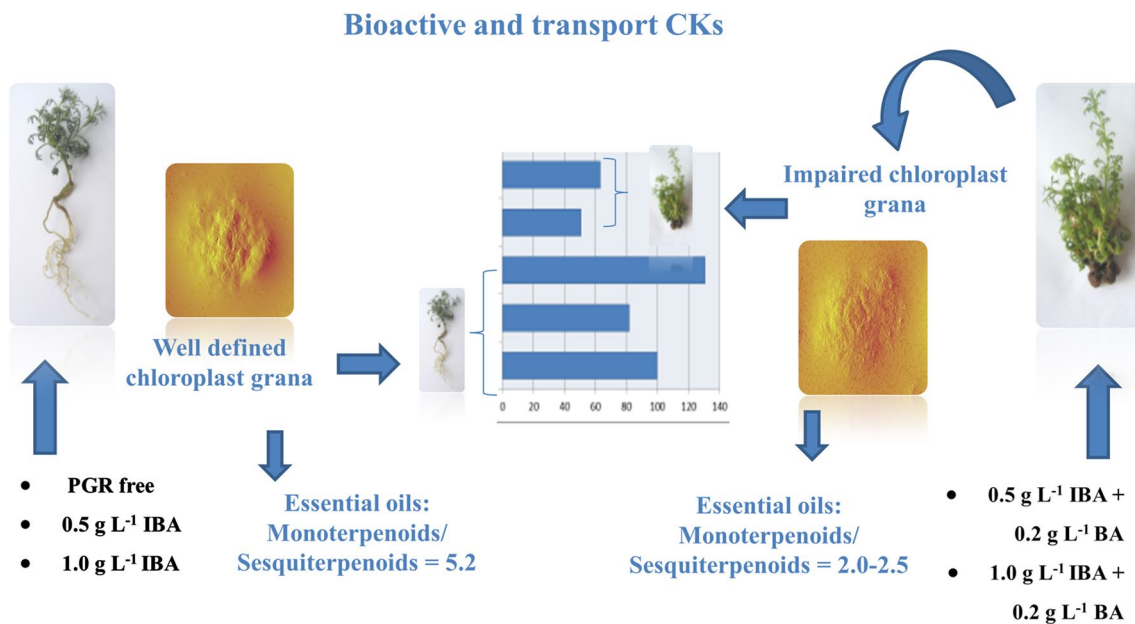


Fig. 8 Schematic representation of the observed interrelations between bioactive and transport isoprenoid cytokinins and monoterpene and sesquiterpene levels in *A. alba* shoots cultures under the effect of exogenous PGR treatments

was obtained by the combination of the two above described IBA concentrations with 0.2 mg L⁻¹ BA. This led to a significant impact on plant morphology—rooting was inhibited and intensive callusogenesis was observed instead (with only rare indirect root formation). Significant alterations of the lateral organization of Photosystem II and chloroplast architecture were also established for the second group of plants, as compared with the first one. Then, the second system exhibited also a profound drop in the monoterpene/sesquiterpene ratio of the essential oils of the aerals (2.5 and 2.0 for GAIP_3 and GAIP_4, respectively) as compared with the first group (monoterpene/sesquiterpene ratio 5.2). Further investigations have also shown an alteration of bioactive plus transport isoprenoid CK levels, as well as *transZ/cisZ* ratio in the second group of plants as compared with plants of the first group (PGR-free control and IBA treated). Two biosynthetic pathways for isoprenoid biosynthesis are present in plants. The mevalonate pathway which is found in the cytoplasm (responsible for sesquiterpenoids, as well as *cisZ* biogenesis) and the MEP pathway, only present in the plastids (strongly linked to photosynthesis and responsible for isoprenylation as well as for monoterpene and *transZ* CKs biogenesis) (Wildermuth and Fall 1998; Bouvier and others 2005; Nagegowda 2010). In addition, amongst their multiple vital roles in cell division, shoot and root development, leaf morphogenesis, flowering, fruiting and seed formation, CKs are responsible for stabilization of the photosynthetic machinery of plants (Vankova 2014).

To conclude, the observed relations suggest a possible interplay between isoprenoid endogenous CKs and terpene

biosynthesis by means of affecting plastid architecture and possible alteration of the efficacy of the biogenetic pathways, spatially situated in the chloroplast (Fig. 8).

Acknowledgements We are thankful to the Swiss Enlargement Contribution in the framework of the Bulgarian-Swiss Research Programme (BSRP, Grant Nos. IZEBZ0_142989; DO2-1153) and Dr. Evelyn Wolfram for PhytoBalk project coordination, the Joint Scientific Research Project between the CAS and BAS (Reg. No. 17-17); the Czech Science Foundation (16-14649S) and we are very grateful to Prof Alessandra Braca for critical reading of the manuscript and complex revision of the scientific English.

Compliance with Ethical Standards

Conflict of interest The authors declare that they have no conflict of interest.

References

- Adams RP (2009) Identification of essential oil components by gas chromatography/mass spectrometry, 4th ed. Allured Busin. Med., Carol Stream
- Albertsson PÅ (2001) A quantitative model of the domain structure of the photosynthetic membrane. Trends Plant Sci 6:349–354
- Andrzhijevskaya EG, Chojnicka A, Bautista JA, Diner BA, van Grondelle R, Dekker JP (2005) Origin of the F685 and F695 fluorescence in photosystem II. Photosynth Res 84:173–180
- Arnon DI (1949) Copper enzymes in isolated chloroplasts. Polyphenol oxidase in *Beta vulgaris*. Plant Physiol 24:1–15
- Bajaj YPS, Furmanowa M, Olszowska O (1988) Biotechnology of the micropropagation of medicinal and aromatic plants. In: Bajaj YPS (eds) Biotechnology in agriculture and forestry, medicinal and aromatic plants I, vol 4. Springer, Berlin, pp 60–103

- Bishopp A, Lehesranta S, Vatén A, Help H, El-Showk S, Scheres B, Helariutta K, Mähönen AP, Sakakibara H, Helariutta Y (2011) Phloem-transported cytokinin regulates polar auxin transport and maintains vascular pattern in the root meristem. *Curr Biol* 21:927–932
- Bouvier F, Suire C, d'Harlingue A, Backhaus RA, Camara B (2000) Molecular cloning of geranyl diphosphate synthase and compartmentation of monoterpene synthesis in plant cells. *Plant J* 24:241–252
- Bouvier F, Rahier A, Camara B (2005) Biogenesis, molecular regulation and function of plant isoprenoids. *Prog Lipid Res* 44:357–429
- Chu HY, Wegel E, Osbourn A (2011) From hormones to secondary metabolism: the emergence of metabolic gene clusters in plants. *Plant J* 66:66–79
- Danova K (2014) Biotechnological utilization of the indigenous biosynthetic capacity of medicinal and aromatic plants. Experience in the genera *Hypericum*, *Pulsatilla* and essential oil bearing *Artemisia alba* characteristic for the Balkan region. In: Govil (ed) *Biotechnology and genetic engineering II*. Studium Press LLC, Houston, pp 355–392
- Danova K, Todorova M, Trendafilova A, Evstatieva L (2012) Cytokinin and auxin effect on the terpenoid profile of the essential oil and morphological characteristics of shoot cultures of *Artemisia alba*. *Nat Prod Commun* 7:1–2
- Dekker JP, Hassoldt A, Pettersson A, Van Roon H, Groot ML, van Grondelle R (1995) On the nature of the F695 and F685 emission of photosystem II. In: Mathis P (ed) *Photosynthesis: from light to biosphere*. Kluwer, Dordrecht, pp 53–56
- Djilianov DL, Dobrev PI, Moyankova DP, Vaňková R, Georgieva DT, Gajdošová S, Motyka V (2013) Dynamics of endogenous phytohormones during desiccation and recovery of the resurrection pulant species *Haberlea rhodopensis*. *J Plant Growth Regul* 32:564–574
- Dobránszki J, Mendler-Drienyovszki N (2014) Cytokinin-induced changes in the chlorophyll content and fluorescence of *in vitro* apple leaves. *J Plant Phys* 171:1472–1478
- Dobrev PI, Kamínek PM (2002) Fast and efficient separation of cytokinins from auxin and abscisic acid and their purification using mixed-mode solid-phase extraction. *J Chromatogr A* 950:21–29
- Dwivedi S, Vaňková R, Motyka V, Herrera C, Žizková E, Auer C (2010) Characterization of *Arabidopsis thaliana* mutant *ror-1* (roscovetine-resistant) and its utilization in understanding of the role of cytokinin *N*-glucosylation pathway in plants. *Plant Growth Regul* 61:231–242
- Gajdošová S, Spíchal L, Kamínek M, Hoyerová K, Novák O, Dobrev PI, Galuszka P, Klíma P, Gaudinová A, Zizková E, Hanus J, Dancák M, Trávníček B, Pesek B, Krupicka M, Vanková R, Strnad M, Motyka V (2011) Distribution, biological activities, metabolism, and the conceivable function of cis-zeatin-type cytokinins in plants. *J Exp Bot* 62:2827–2840
- Gobets B, van Grondelle R (2001) Energy transfer and trapping in photosystem I. *Biochim Biophys Acta* 1507:80–99
- Harrison MA, Melis A (1992) Organization and stability of polypeptides associated with the chlorophyll a-b light-harvesting complex of photosystem-II. *Plant Cell Physiol* 33:627–637
- Hirose N, Takei K, Kuroha T, Kamada-Nobusada T, Hayashi H, Sakakibara H (2008) Regulation of cytokinin biosynthesis, compartmentalization and translocation. *J Exp Bot* 59:75–83
- Ikeuchi M, Sugimoto K, Iwase A (2013) Plant callus: mechanisms of induction and repression. *Plant Cell* 25:3159–3173
- Kakimoto T (2003) Perception and signal transduction of cytokinins. *Ann Rev Plant Biol* 54:605–627
- Kamínek M, Březinová A, Gaudinová A, Motyka V, Vaňková R, Zažímalová E (2000) Purine cytokinins: a proposal for abbreviations. *Plant Growth Regul* 32:253–256
- Kasahara H, Takei K, Ueda N, Hishiyama S, Yamaya T, Kamiya Y, Yamaguchi S, Sakakibara H (2004) Distinct isoprenoid origins of *cis*- and *trans*-Zeatin biosyntheses in *Arabidopsis*. *J Biol Chem* 279:14049–14054
- Ko D, Kang J, Kiba T, Park J, Kojima M, Do J, Kim KY, Kwon M, Ender A, Song WY, Martinoia E, Sakakibara H, Lee Y (2014) *Arabidopsis* ABCG14 is essential for the root-to-shoot translocation of cytokinin. *Proc Natl Acad Sci USA* 111:7150–7155
- Kovács L, Damkjær J, Kerešiče S, Illoiaia C, Ruban AV, Boekema EJ, Jansson S, Horton P (2006) Lack of the light-harvesting complex CP24 affects the structure and function of the grana membranes of higher plant chloroplasts. *Plant Cell* 18:3106–3120
- Krumova S, Motyka V, Dobrev P, Todorova M, Trendafilova A, Evstatieva L, Danova K (2013) Terpenoid profile of *Artemisia alba* is related to endogenous cytokinins *in vitro*. *Bul J Agric Sci* 19:26–30
- Kudo T, Kiba T, Sakakibara H (2010) Metabolism and long-distance translocation of cytokinins. *J Integr Plant Biol* 52:53–60
- Lomin SN, Krivosheev DM, Steklov MY, Arkhipov DV, Osolodkin DI, Schmulling T, Romanov GA (2015) Plant membrane assays with cytokinin receptors underpin the unique role of free cytokinin bases as biologically active ligands. *J Exp Bot* 66:1851–1863
- Mc Garvey D, Croteau R (1995) Terpenoid metabolism. *Plant Cell* 7:1015–1026
- Mullet JE, Burkner JJ, Arntzen CJ (1980) Chlorophyll proteins of photosystem I. *Plant Physiol* 65:814–822
- Nagegowda DA (2010) Plant volatile terpenoid metabolism: biosynthetic genes, transcriptional regulation and subcellular compartmentation. *FEBS Lett* 584:2965–2973
- Pribil M, Labs M, Leister D (2014) Structure and dynamics of thylakoids in land plants. *J Exp Bot* 65:1955–1972
- Radulović N, Blagojević P (2010) Volatile profiles of *Artemisia alba* from contrasting serpentine and calcareous habitats. *Nat Prod Commun* 5:1117–1122
- Roberts SC (2007) Production and engineering of terpenoids in plant cell culture. *Nat Chem Biol* 3:387–395
- Sakakibara H (2006) Cytokinins: activity, biosynthesis, and translocation. *Annu Rev Plant Biol* 57:431–449
- Sandra P, Bicchì C (1987) Microtechniques in essential oil analysis. In: Sandra P, Bicchì C (eds) *Capillary gas chromatography in essential oil analysis*. Huethig, New York, pp 85–122
- Seemann M, Bui BTS, Wolff M, Miginiac-Maslow M, Rohmer M (2006) Isoprenoid biosynthesis in plant chloroplasts via the MEP pathway: direct thylakoid/ferredoxin-dependent photoreduction of GcpE/IspG. *FEBS Lett* 580:1547–1552
- Skoog F, Miller CO (1957) Chemical regulation of growth and organ formation in plant tissues cultured *in vitro*. *Symp Soc Exp Biol* 11:118–130
- Takei K, Yamaya T, Sakakibara H (2004) *Arabidopsis* CYP735A1 and CYP735A2 encode cytokinin hydroxylases that catalyze the biosynthesis of *trans*-Zeatin. *J Biol Chem* 279:41866–41872
- Tkachev AV (2008) Investigation of volatile compounds in plants. Offset, Novosibirsk
- Trendafilova A, Todorova M, Vitkova A (2010) Essential oil composition of *Achillea clusiana* from Bulgaria. *Nat Prod Commun* 5:129–132
- Vankova R (2014) Cytokinin regulation of plant growth and stress responses. In: Tran LSP, Pal S (eds) *Phytohormones: a window to metabolism, signaling and biotechnological applications*. Springer, New York
- Werner T, Motyka V, Strnad M, Schmülling T (2001) Regulation of plant growth by cytokinin. *Proc Natl Acad Sci USA* 98:10487–10492
- Werner T, Motyka V, Laucou V, Smets R, van Onckelen H, Schmülling T (2003) Cytokinin-deficient transgenic *Arabidopsis* plants show multiple developmental alterations indicating opposite functions

- of cytokinins in the regulation of shoot and root meristem activity. *Plant Cell* 15:2532–2550
- Wildermuth MC, Fall R (1998) Biochemical characterization of stromal and thylakoid-bound isoforms of isoprene synthase in willow leaves. *Plant Physiol* 116:1111–1123
- Záveská Drábková L, Dobrev PI, Motyka V (2015) Phytohormone profiling across the bryophytes. *PLoS ONE* 10:e0125411
- Žižková E, Dobrev PI, Muhovski Y, Hošek P, Hoyerová K, Haisel D, Procházková D, Lutts S, Motyka V, Hichri I (2015) Tomato (*Solanum lycopersicum* L.) SHPT3 and SHPT4 isopentenyltransferases mediate salt stress response in tomato. *BMC Plant Biol* 15:85